Investigation of sea skin surface effects and sea surface emissivity effects based on thermal infrared camera image

Sumio TAMBA
Center for Computer and Communications, Hirosaki University
3, Bunkyo-cho, Hirosaki, Aomori 036-8561, Japan
tanba@cc.hirosaki-u.ac.jp

Kyu YOSHIMORI, and Kazuya INOMATA
Department of Computer and Information Science, Faculty of Engineering, Iwate University
4-3-5 Ueda, Morioka, Iwate 020-8551, Japan

Abstract: Sea surface temperatures (SSTs) estimated from satellite data are affected by various kinds of disturbance factors. In order to accurately estimate SSTs based on radiometric data observed by satellite, it is important to correct the effects by these disturbance factors. We obtained a huge data set of skin sea surface temperature images observed by a thermal infrared camera (TIC) in MUBEX Campaign. TIC installed on an observation vessel recorded sea surface skin temperature distribution under various weather conditions. Based on some special images observed by TIC, we estimated skin effects and effective sea surface emissivity. In this paper, we report the methods and results of these estimations.

I. INTRODUCTION

Atmospheric effects are well known as one of dominant error factors to estimate SSTs from space. However, other disturbance factors also affect the SST estimation. Skin sea surface effects[1] and emissivity effects[2, 3] are respectively regarded as one of disturbance factors. The skin sea surface effects are defined as the temperature differences between the skin sea surface and sub-surface bulk water. The emissivity effects originated from the use of improper value of sea surface emissivity. Usually, a value of sea surface emissivity is assumed as unity, but real value of the emissivity is rather small. The skin sea surface effects and the sea surface emissivity are hard to measure in field.

We planed an observation project named as the Mutsu-bay sea surface temperature validation experiment (MUBEX)[4, 5] to obtain reliable observation data on the sea. As shown in Fig. 1, Various kinds of devices to observe sea and weather conditions were used in MUBEX, which was held in Mutsu Bay at the northern end of Honshu Island, Japan, during 1995 and 1997. A thermal infrared camera (TIC) was used as one of important observation devices in MUBEX Campaign. The TIC installed on an

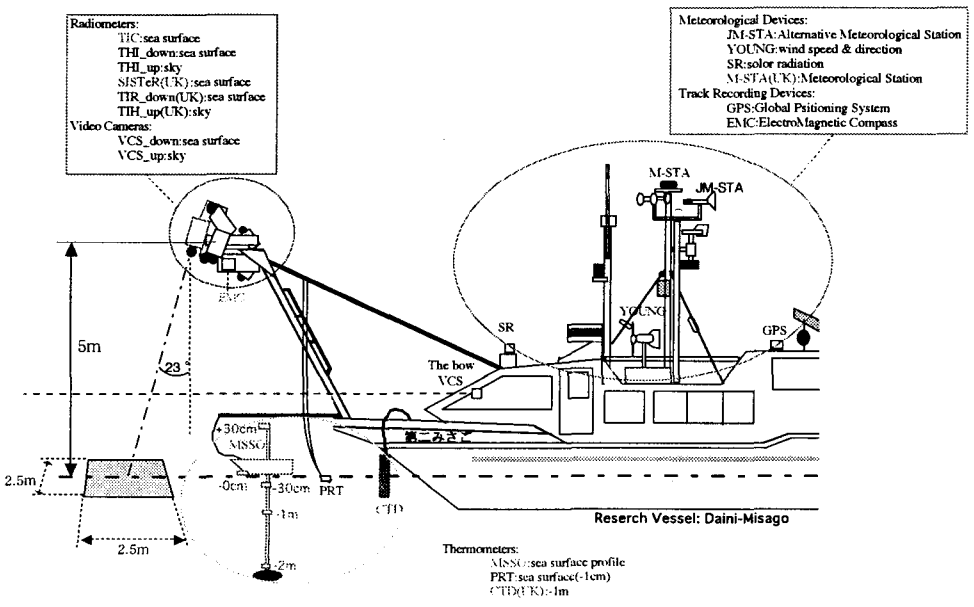

Fig. 1 Instrumentation on the observation vessel of MUBEX '97

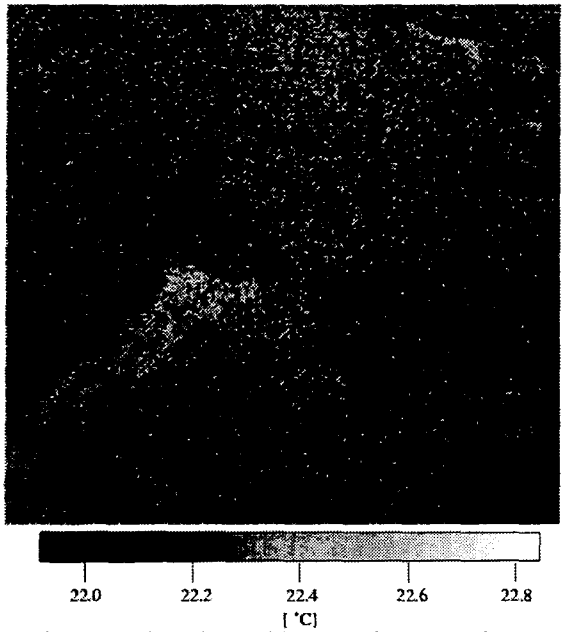

Fig. 2 Typical thermal image of a sea surface in which whitecaps are observed.

observation vessel observes sea surface skin temperature distribution of an area of 2.5 m by 2.5 m.

We obtained some thermal images at the same time when whitecaps appeared in visible images. Temperature in a region that whitecaps appeared is warmer than other regions. This means whitecaps break a skin surface layer, which covers a sea surface with a thickness of about 10 micro meters, so that warmer water appeared. For this analysis, 31 thermal images including whitecaps were selected. We estimated temperature difference in the skin surface layer based on these TIC images statistically.

We also obtained some images collected under a special weather condition, which means a clear sky accompanying some clouds, a weak wind velocity, and a flat sea surface like a mirror surface. These images include reflection of downward radiation from cloud at the sea surface. The region with the reflection shows higher temperature than an ordinary region without it. This effect is caused when a target is non-blackbody. It is possible to estimate sea surface emissivity based on these images. First, we picked up five images including the reflection. Secondly, for the five images, a temperature difference between the region with higher temperature and the ordinary region was calculated. Finally, a sea surface emissivity was calculated by using Planck's function based on the difference.

In this paper, we report a statistical value of estimated temperature difference in the skin surface layer, also a statistical value of estimated sea surface emissivity. The former means sea skin surface effects, and the latter means sea surface emissivity effects.

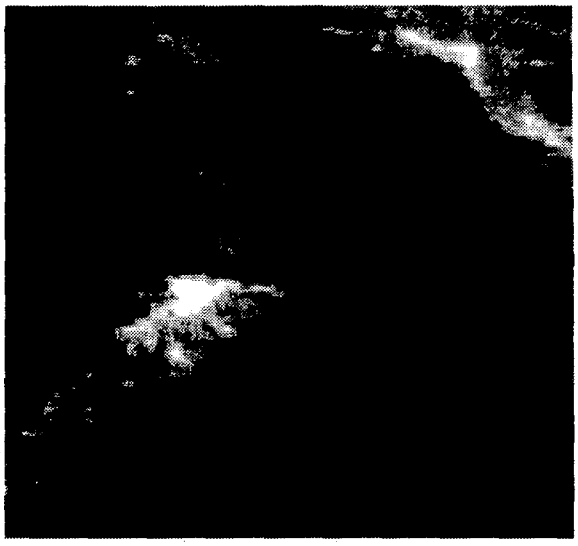
Fig. 3 A synchronized visible image which corresponds to the thermal image in Fig. 1.

II. SKIN SEA SURFACE EFFECTS

Preparation

This analysis is based on 82,000 scenes of the thermal image of sea surface. These images are coupled with visible video movies and the meteorological and environmental data measured simultaneously with obtaining the images. The data were acquired during MUBEX campaign held partly on July 19-25 in 1997.

Figure 2 is an example of infrared sea surface image obtained by the thermal infrared camera (TIC), when dynamic whitecaps are observed in a series of visible video images. Specifications of TIC are shown in Table 1. Since the scanning time of TIC is 1 second while the frame rate of video camera is 30 fps, patterns of temperature distribution in thermal images and patterns of visible whitecaps in video do not coincide in general. We then interpolate and resample the 30 video images in accordance with the scanning rate of TIC.

The result is shown in Fig. 3, and we see an apparent coincidence of relatively-high temperature patterns in Fig. 2 and whitecaps in Fig. 3. The temperature in whitecaps area somehow represents the temperature of sub-surface bulk water just below the skin layer. This fact indicates that the skin sea surface temperature difference can be extracted from the single thermal image of a sea surface by

Table1 Specification of TIC and THI.

	TIC	THI
Temperature Range	20~80 deg.C	-50~500 deg.C
Temperature Resolution	0.075 deg.C	0.1 deg.C
Wave Length	8~13 μm	8~12 μm
IFOV	1.5 m rad	8.5 deg.
FOV	(H)30 deg. x (V)28.5 deg.	8.5 deg.

comparing the temperature in whitecaps area with the temperature in ordinary sea surface having skin boundary layer.

Method

We choose 31 pairs of infrared image of sea surface and resampled visible image where the correspondence of whitecaps patterns with temperature distribution is clearly observed. Then, in order to extract the skin sea surface temperature difference from each thermal image, we divide the image into three parts: skin sea surface area, breaking boundary layer area, and intermediate area. For this purpose, we introduce the following threshold temperatures:

$$T_{tbulk} = T_{smax} - n\sigma, \quad (1)$$

$$T_{tskin} = T_{tbulk} - \sigma/3. \quad (2)$$

Here, T_{tbulk} is the lowest temperature of sub-surface bulk water which is observed by breaking, T_{tskin} is the highest temperature of the skin sea surface, T_{smax} and σ are the maximum and standard deviation of sea surface temperature over the thermal image. In Eq. (1), n represents a parameter for adjusting the threshold and 1/3 value in Eq. (2) is determined such that the area having temperatures lower than T_{tskin} is regarded as indeed the skin region. This value is suited for our 31 data sets. A divided sea surface is shown in Fig. 4. Note that the area having temperature between T_{tbulk} and T_{tskin} is regarded as that of insufficient boundary layer breaking and, then, excluded from either area.

Results

We now define the skin sea surface temperature difference ΔT_{skin} as the difference of the average temperature T_{skin} in skin sea surface area from the average temperature in breaking area T_{bulk}:

$$\Delta T_{skin} = T_{skin} - T_{bulk}. \quad (3)$$

The statistics of ΔT_{skin} over 31 samples are summarized in Table 2.

Table 2 Statistics of ΔT_{skin} over 31 data sets

	[deg.C]			
n	mean	s.d.	max.	min.
31	-0.137	0.023	-0.089	-0.183

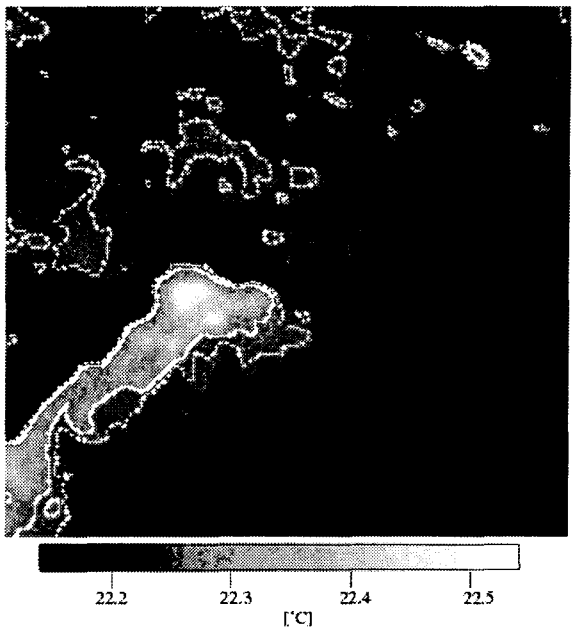

Fig. 4 This image is a result divided into whitecaps areas and skin sea surface areas, which is obtained by applying the smoothing and the temperature thresholdning technique based on Eqs. (1) and (2), with parameter $n = 1.85$.

III. SEA SURFACE EMISSIVITY EFFECTS

Background

Many research results on the atmospheric effects that are the largest in these disturbances have been reported. However, in radiative transfer model used for correction of atmospheric effects, emissivity of a sea surface is usually assumed to be unity. Theoretical value of emissivity of a water surface is calculated from its spectral refractive index[6], however, it is in general a hard task to measure the effective emissivity of a real sea surface under various environmental conditions. If the actual value of sea surface emissivity is known at a satellite observation, the correction for a SST is possible. It is expected that the accuracy of the SST derived from satellite data is greatly improved.

On the basis of MUBEX observation data obtained during the summer of 1997, we have already reported a technique to determinate the effective emissivity of a sea surface from a thermal image, in which sea surface and a reference target are included simultaneously[7]. In this section, we will introduce alternative technique to calculate the effective emissivity of a sea surface. The present method uses temperature images of a sea surface obtained under inhomogeneous clouds distributions. To get a better result, we choose a special weather condition: a calm sea surface appeared under a state of windlessness.

Model

Let us now consider a situation in which we observe a calm sea surface underlying a clear sky with an inhomogeneous cloud distribution. In this case, the obtained sea surface image reveals an image of that cloud distribution, since every element of a sea surface partially reflects the sky radiation, as well as it emanates the thermal emission according to its temperature. The sea surface image is, then, separated into two parts: the region that reflects the clear sky (region 1) and the region for clouds (region 2). Let the brightness temperature of the sea surface in region 1 be T_{r_sky} and let the brightness temperature in region 2 be T_{r_cloud}, we obtain an equation to estimate the sea surface emissivity from the thermal image of a sea surface:

$$\varepsilon_\lambda = 1 - (B_\lambda(T_{r\_cloud}) - B_\lambda(T_{r\_sky}))/(B_\lambda(T_{cloud}) - B_\lambda(T_{sky})) \quad (4)$$

where λ is the wavelength of the observed thermal radiation, T_{sky} and T_{cloud} are, respectively, the brightness temperature of the clear sky and clouds, ε_λ being the spectral emissivity of the sea surface, $B_\lambda(T)$ is the spectral radiance of a blackbody with temperature T, and T the skin sea surface temperature, which is assumed to be the same in both 1 and 2 regions. We note that, although not demonstrated here, the skin sea surface temperature T can also be determined simultaneously from this thermal image, as the same manner as reported before[7].

Used Data

As shown in Figure 1, a TIC was installed on an observation stage about 5m height made at the bow of the vessel with a tilt angle of 23 degrees to the forward direction of the vessel. A spot type thermal infrared radiometer (THI) made by tasco co. is also used for a sky temperature observation, which was installed on the stage with a zenith angle of 23 degrees to the forward direction of the vessel. A downward radiance entering the sea surface can be measured by this THI. The Observation intervals of TIC and THI were one second together. Specifications of TIC and THI are shown in Table 1. In addition, the vessel carried a Moving type Sea Surface Observer (MSSO) for a meteorological observation, which measures SSTs at four depths (0cm, 30cm, 1m, and 2m) and air temperature at 30 cm.

We selected five TIC images provided from 2:56:51 to 2:56:55 on July 21, 1997 for this analysis. Figure 3 shows these five images. In addition, we obtained environmental parameters for this analysis based on the meteorological observation data.

Processing

Hereafter, the five images shown in Figure 3 are called with image (A) to (E) in order of acquisition time. These five images were acquired in an interval for one second. The warmer region at the right side of each image occurred by radiation from cumulus clouds, and we can find a patch region with the same shape on each image. The warmer area was including reflection from the same cloud. We selected the warmer region (region C) and the region including reflection of a clear sky radiation (region S) on each image.

The selection method is as follows. The region C on each image is extracted by a threshold operation for the histogram of pixel value. The region S is extracted from the left side of each image as the rest of region C, but about 10 pixels width around edge of the region C is removed. This step avoids an effect of cloud edge. In addition, when the number of pixels belonging to each region on each scan line is less than 40, the pixels on the scan line are removed.

Calculation results

In Figure 4, masks to identify the region C and the region S on each image in Figure 3 are shown. Table 3 shows statistics of brightness temperatures in both masks. Table 4 shows the calculation results of sea surface emissivity for each image, also the temperature values used for the calculation. Minimum and maximum of sky temperature were denoted as Tsky and Tcloud, respectively. Figure 5 shows a plot of the sea surface emissivity obtained as a function of zenith angle. The value of zenith angle of each mask was assigned by the zenith angle at the center of the mask. In addition, theoretical values calculated based on the refractive index of water and zenith angle is shown in the figure, for comparison. We found no appreciable dependence of emissivity on the zenith angle. The mean value and standard deviation of the emissivity values are 0.9895

Table 3 Statistic of T_{r_cloud} and T_{r_sky} for each Image.

	id	angles deg.	samples	mean deg. C	s.d. deg. C	max. deg. C	min. deg. C
Tr_cloud	A	35.58	1684	21.215	0.0655	21.51	21.03
	B	31.29	1527	21.253	0.0634	21.53	21.08
	C	24.97	3568	21.292	0.0671	21.54	21.12
	D	16.50	3193	21.316	0.0639	21.56	21.14
	E	11.02	2066	21.331	0.0697	21.63	21.15
Tr_sky	A	35.70	2883	20.974	0.0620	21.16	20.71
	B	31.65	2566	20.999	0.0659	21.17	20.76
	C	25.21	6712	21.052	0.0629	21.23	20.80
	D	16.50	9364	21.088	0.0731	21.31	20.80
	E	11.02	4442	21.087	0.0643	21.26	20.83

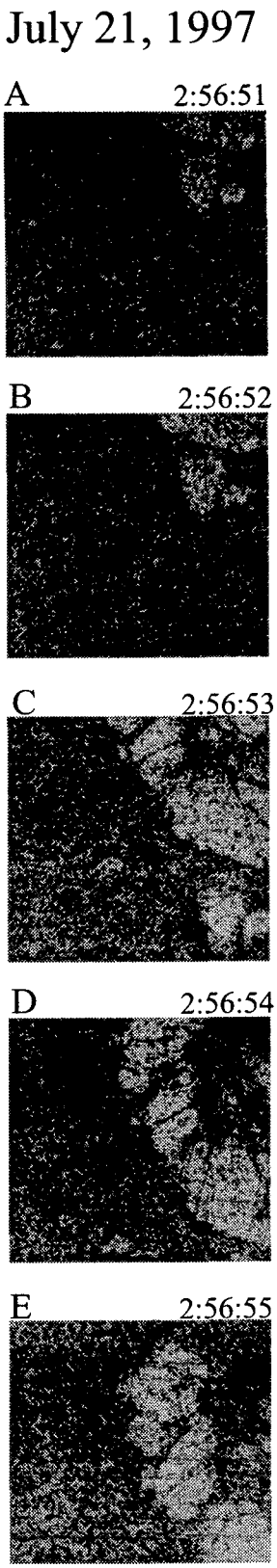

Fig. 3 Original TIC images used for emissivity estimation.

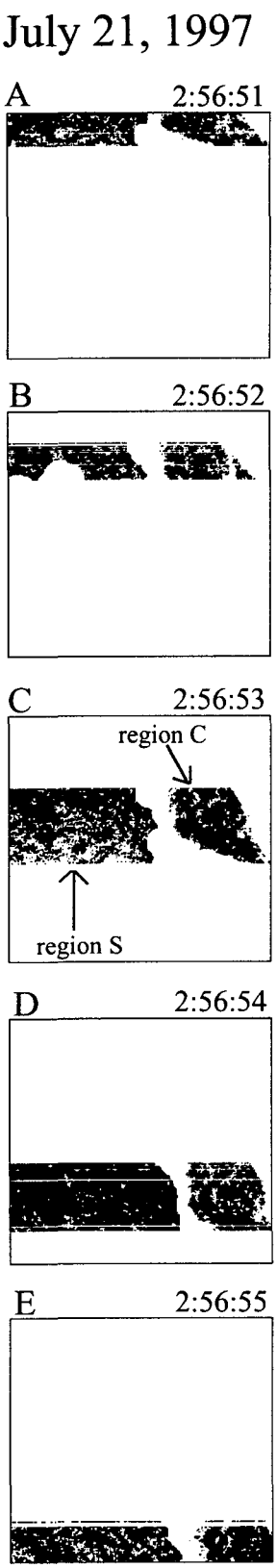

Fig. 4 Mask images obtained from the original images in Fig. 3, which idrntify the region including reflection of cloud radiation and the region including reflection of clear sky radiation.

Table 4 Calculated emissivity and used parameters

id	angles deg.	Tr_cloud deg. C	Tr_sky deg. C	Tcloud deg. C	Tsky deg. C	emissivity
A	35.70	21.215	20.974	12.156	-18.42	0.98952
B	31.65	21.253	20.999	12.156	-18.42	0.98898
C	25.21	21.292	21.052	12.156	-18.42	0.98958
D	16.50	21.316	21.088	12.156	-18.42	0.99004
E	11.02	21.331	21.087	12.156	-18.42	0.98938

and 0.0003, respectively. There is no angle dependence of the emissivity in this figure.

IV. DISCUSSION

The skin surface temperature obtained by this analysis was not so large, but the temperature varied depending on the weather and sea conditions. For more accurate result, it is necessary to increase the number of sample images.

Figure 5 shows the discrepancy between the calculated values and the theoretical values of sea surface emissivity. The mean value and standard deviation of the difference are 0.0013 and 0.0006, and the former value means that the calculated value is greater than the theoretical one by 0.13 %.

Figure 6 shows a relationship between the error of emissivity and Tr_cloud. In the case of Tr_sky, almost similar results are provided. The curve in Figure 6 shows that the

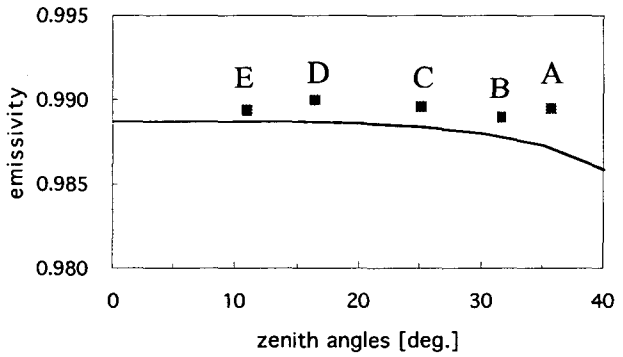

Fig. 5 Relationship between scan angle and emissivity calculated from each image.

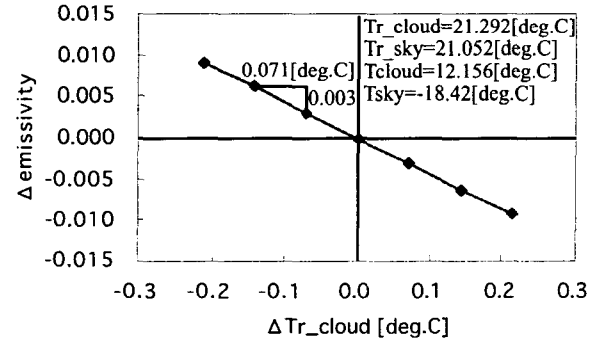

Fig. 6 Relationship between ΔT_{r_cloud} and Δemissivity.

emissivity error of about 0.003 (0.3 %) appears when measurements by TIC include an error of 0.071 deg.C. The value of 0.071 deg.C corresponds to the accuracy of TIC data after removing dominant noise[8]. From these results, the discrepancy between the theoretical value and the calculated value based on the observation data is able to be ignored at a viewpoint of the specification of the measurement devices. In addition, the results suggest a guideline to measure emissivity with a high accuracy.

V. CONCLUDION

We have investigated the skin sea surface effects and the sea surface emissivity effects based on the data sets obtained by Mutsu-bay sea surface temperature validation experiment (MUBEX) held in 1997. We found the magnitude of the skin sea surface effects by the statistical analysis of many thermal images observed by TIC. Effective sea surface emissivity was estimated on the basis of SST image data measured by TIC and sky temperature data measured by THI under the special weather conditions. This means that the measurement of effective emissivity is possible in field without using reference targets under the special conditions.

REFERENCES

[1] R. Yokoyama, S. Tamba and T. Souma, "Sea surface effects on the sea surface temperature estimation by remote sensing," Int. J. Remote Sensing, vol. 16, pp. 227-238, 1995.

[2] Kyu Yoshimori, Sumio Tamba, and Ryuzo Yokoyama, "On-sight measurement of skin sea surface temperature and sea surface emissivity from a single thermal imagery," Proc. IGARSS, CD, 2001.

[3] Sumio Tamba, Kyu Yoshimori, and Ryuzo Yokoyama, "Estimation of effective sea surface emissivity based on TIC data," Proc. IGARSS, CD, 2001.

[4] R. Yokoyama, S. Tamba, T. Souma, D. Llewellyn-Jones, and I. M. Parks "MUBEX: Japan and U.K. collaboration for Mutsu Bay sea surface validation experiment," Proc. IGARSS, pp. 311-313, 1997.

[5] I. M. Parkes, T. N. Sheasby, D. T. Llewellyn-Jones, T. J. Nightingale, A. M. Zavody, C. T. Mutlow, R. Yokoyama, S. Tamba, and C. J. Donlon, "The Mutsu Bay Experiment: validation of ATSR-1 and ATSR-2 sea surface temperature," Int. J. Remote Sensing, vol. 21, pp. 3445-3460, 2000.

[6]G. M. Hale and M. R. Querry, Optical constants of water in the 200-nm to 200-mm wavelength region, Appl. Opt. Vol. 12, 555-563 , 1973.

[7]K. Yoshimori, S. Tamba and R. Yokoyama, Simultaneous measurements of skin sea surface temperature and sea surface emissivity from a single thermal imagery, Vol. 41, No. 24, Appled Optics, pp.4937-4944,2002.

[8]S. Tamba, R. Yokoyama, Line noise extraction of thermal infrared camera image in observing sea skin temperature, Proc. IGARSS'97, pp.305-307, 1997.